

1 The fate of Zn in agricultural soils: A stable isotope approach to  
2 anthropogenic impact, soil formation and soil-plant cycling

3 Martin Imseng,<sup>1</sup> Matthias Wiggnerhauser,<sup>2</sup> Michael Müller,<sup>3</sup> Armin Keller,<sup>3</sup> Emmanuel  
4 Frossard,<sup>2</sup> Wolfgang Wilcke,<sup>4</sup> Moritz Bigalke<sup>1\*</sup>

5 <sup>1</sup>Institute of Geography, University of Bern, Hallerstrasse 12, 3012 Bern, Switzerland

6 <sup>2</sup>Institute of Agricultural Sciences, ETH Zurich, Eschikon 33, 8315 Lindau, Switzerland

7 <sup>3</sup>Swiss Soil Monitoring Network (NABO), Agroscope, Reckenholzstrasse 191, 8046 Zürich,  
8 Switzerland

9 <sup>4</sup>Institute of Geography and Geoecology, Karlsruhe Institute of Technology (KIT), Reinhard-  
10 Baumeister-Platz 1, 76131 Karlsruhe, Germany

11 \*Corresponding author: Moritz Bigalke, [moritz.bigalke@giub.unibe.ch](mailto:moritz.bigalke@giub.unibe.ch), tel. +41(0)316314055

12

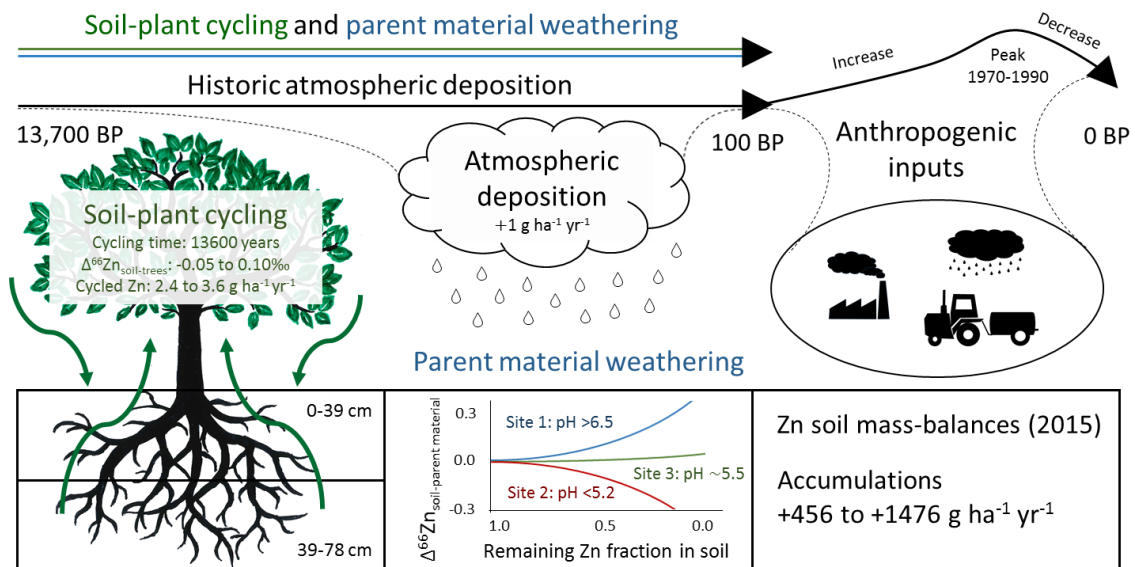
13 **Abstract**

14 The supplementation of Zn to farm animal feed and the excretion via manure leads to an  
15 unintended Zn input to agricultural systems, which might compromise the long-term soil  
16 fertility. The Zn fluxes at three grassland sites in Switzerland were determined by a detailed  
17 analysis of relevant inputs (atmospheric deposition, manure, weathering) and outputs  
18 (seepage water, biomass harvest) during one hydrological year. The most important Zn input  
19 occurred through animal manure (1,076 to 1,857 g ha<sup>-1</sup> yr<sup>-1</sup>) and Zn mass balances revealed  
20 net Zn accumulations (456 to 1,478 g ha<sup>-1</sup> yr<sup>-1</sup>). We used Zn stable isotopes to assess the  
21 importance of anthropogenic impacts and natural long-term processes on the Zn distribution  
22 in soils. Soil-plant cycling and parent material weathering were identified as the most  
23 important processes, over the entire period of soil formation (13,700 years), while the soil pH  
24 strongly affected the direction of Zn isotopic fractionation. Recent anthropogenic inputs of Zn  
25 only had a smaller influence compared to the natural processes of the past 13,700 years.  
26 However, this will probably change in the future, as Zn stocks in the 0-20 cm layer will  
27 increase by 22% to 68% in the next 100 years, if Zn inputs remain on the same level as today.

28

29

30 **TOC ART**



31

32 **Introduction**

33 In intensive agriculture, Zn is supplemented to farm animal feed and veterinary drugs to  
34 ensure optimal growth and promote wound healing, respectively.<sup>1,2</sup> Feed additives were  
35 increasingly supplied to farm animals after intensification of agricultural practices in the 20<sup>th</sup>  
36 century.<sup>3,4</sup> A major part of the Zn is excreted and brought to the field with manure  
37 application.<sup>5-9</sup> In the European Union Zn inputs with manure currently range from 300 to  
38 2,700 g ha<sup>-1</sup> yr<sup>-1</sup>.<sup>10-12</sup> This Zn might accumulate in soils and compromise the growth of  
39 microorganisms, invertebrates, and plants.<sup>13,14</sup>

40 In uncontaminated environments, Zn is naturally introduced to soils by the weathering of  
41 parent materials. The bioavailable and exchangeable Zn<sup>2+</sup> is mainly adsorbed to soil organic  
42 matter and (hydr)oxides, and desorption processes into soil solution depend on the pH  
43 value.<sup>15</sup> Nonspecific sorption to clay minerals and mineral precipitation are important at  
44 elevated Zn concentrations and are only weakly related with the pH value.<sup>15</sup> Typical soil Zn  
45 concentrations range from 10 to 100 mg kg<sup>-1</sup> and correspond to Zn stocks of ~45,000 to  
46 600,000 g ha<sup>-1</sup> in the uppermost 50-cm soil layer. Another relevant Zn source to soils can be  
47 atmospheric deposition. Zn emissions to the atmosphere originate from natural sources like  
48 biological or geogenic particles, volcanoes or forest fires<sup>16</sup> and from human sources like fossil

49 fuel combustion, metal production, and refuse incineration.<sup>17</sup> In Europe, anthropogenic Zn  
50 emissions increased during the 20<sup>th</sup> century, peaked in 1965-1970 with ~30x higher  
51 deposition rates than natural background deposition rates, and decreased thereafter.<sup>18,19</sup>  
52 Recent studies have reported atmospheric deposition rates between 20 and 540 g ha<sup>-1</sup> yr<sup>-1</sup> in  
53 13 European countries.<sup>20</sup>

54 The dominant Zn outputs from agricultural soils are leaching with seepage water and crop  
55 harvest. Zinc concentrations in soil solution can be estimated with the help of soil-water  
56 partition coefficients ( $K_d$  values) which predict an increase of dissolved Zn concentrations by a  
57 factor of 5 per unit pH decrease.<sup>21</sup> For European soils, leaching rates between 18 and 135 g  
58 ha<sup>-1</sup> yr<sup>-1</sup> have been reported.<sup>11,12,22,23</sup> The Zn outputs with harvest mainly depend on crop  
59 type, soil productivity and soil Zn concentrations with reported values for European soils  
60 between 30 and 540 g ha<sup>-1</sup> yr<sup>-1</sup>.<sup>10-12,23</sup>

61 Natural abundance stable isotope compositions are a tool that is increasingly used to  
62 differentiate between geogenic and anthropogenic sources.<sup>24</sup> Igneous and sedimentary rocks  
63 show limited variations in their isotopic compositions ( $\delta^{66}\text{Zn} = -0.22$  to  $0.28$  ‰), except  
64 carbonates (0 to  $1.13$  ‰)<sup>25</sup> which can be more enriched in heavy isotopes, caused by the  
65 preferential recycling of isotopically light Zn in the water column by microorganisms. In  
66 contrast, anthropogenic activities cause larger isotopic variability ( $-0.98$  to  $0.53$  ‰) mainly  
67 produced by evaporation and condensation processes of elemental Zn in metal refineries.<sup>26,27</sup>  
68 Because of the distinct isotope composition of geogenic and anthropogenic sources, previous  
69 studies successfully traced Zn contamination sources of soils, such as Zn from smelters,<sup>28</sup> but  
70 also from sources with less isotopic variability like diffuse anthropogenic contamination<sup>29</sup> and  
71 pig slurry.<sup>30</sup> Beside different sources, biogeochemical processes can also produce significant  
72 Zn isotope fractionation in soils and plants.<sup>31,32</sup> The difference in isotope composition  
73 between bulk soil and the plant shoot is a result of isotope fractionation processes during Zn  
74 desorption from the bulk soil into soil solution, Zn speciation in soil solution, Zn plant uptake  
75 and Zn transport from root to shoot. During weathering of biotite granite<sup>33</sup> and sulfide-rich  
76 minerals,<sup>23</sup> leachates showed partly heavier and partly lighter Zn isotopic composition,  
77 compared to the parent rocks. Another study on the formation of aerobic soils on the island  
78 of Maui attributed the slight depletion of the soils in heavy Zn isotopes to permanent leaching  
79 of organic acid-bound Zn.<sup>34</sup> Furthermore, several studies found the preferential inner-sphere

80 adsorption of heavy Zn isotopes onto (hydr)oxides ( $\Delta^{66}\text{Zn}_{\text{aqueous-adsorbed}} = -0.29$  to  $-0.52$  ‰),<sup>35,36</sup>  
81 quartz and amorphous  $\text{SiO}_2$  ( $-0.60$  to  $-0.94$ ‰),<sup>37</sup> calcite ( $-0.41$  to  $-0.73$ ‰),<sup>38</sup> kaolinite ( $-0.49 \pm$   
82  $0.06$ ‰),<sup>39</sup> and high-affinity organic matter sites ( $-0.24 \pm 0.06$ ‰).<sup>40</sup> In contrast, Zn adsorption  
83 as outer-sphere complex and to low affinity organic matter sites exhibited much smaller or no  
84 isotopic fractionation.<sup>37,39,40</sup> Soil leachates showed distinct isotopic fractionation. While 0.1 M  
85 HCl extracts were mostly isotopically heavier than the respective agricultural bulk soils, 0.01  
86 M  $\text{CaCl}_2$  extracts were isotopically lighter than plant-free Zn-contaminated bulk soils  
87 ( $\Delta^{66}\text{Zn}_{\text{extract-soil}} = -0.07$  to  $-0.25$ ‰),<sup>41,42</sup> but became isotopically heavier in the presence of  
88 plants. The latter was explained by plant-induced soil acidification and mobilization of the  
89 (hydr)oxide-bound Zn pool.<sup>41,43,44</sup> In soils with sufficient Zn supply, plant shoots were more  
90 enriched in light isotopes than plant-available soil pools,<sup>41,42,45,46</sup> but partly more enriched in  
91 heavy isotopes than bulk soils.<sup>46,47</sup> This variation can be explained by plant-induced Zn  
92 mobilization (isotopically heavy), low-affinity Zn uptake (isotopically neutral to light),  
93 complexation, and storage of excessive cytosol Zn in vacuoles of root cells (isotopically heavy),  
94 and the Zn transport to the shoot through efflux transporters (isotopically light).<sup>32,48</sup>

95 Several studies established Zn mass balances for agricultural soils and identified manure as  
96 the most important input which leads to net Zn accumulations in European soils.<sup>11,20,49–51</sup>  
97 Nevertheless, these studies did not include fluxes with atmospheric deposition and seepage  
98 water or estimated them with model predictions. Fekiacova et al.<sup>30</sup> hypothesized that  
99 isotopically heavier topsoils were related to past pig slurry inputs. However, the study partly  
100 used literature data and did not measure isotope compositions of all relevant system fluxes.<sup>30</sup>

101 The addition of Zn from the atmosphere or via manure results in a preferential accumulation  
102 of Zn in the topsoil, because of the low Zn mobility in most soils. Therefore, Zn accumulation  
103 in the A horizon relative to the subsoil and parent material is usually interpreted as indication  
104 of anthropogenic metal accumulation.<sup>52,53</sup> However, in recent work we have shown that the  
105 accumulation of Cd in topsoils of three Swiss arable soils mainly originated from natural soil-  
106 plant cycling during the whole Holocene<sup>54</sup> as also described for growth-limiting plant  
107 nutrients.<sup>55,56</sup>

108 Here, we used *in situ* measured data to establish Zn mass balances for three grassland sites.  
109 Soil Zn concentrations and relevant Zn inputs (atmospheric deposition, manure, weathering  
110 of parent material) and outputs (seepage water, grassland harvest) were determined during

111 one hydrological year, from May 2014 to May 2015. Additionally, natural variations in Zn  
112 stable isotope compositions were used to trace sources and to investigate processes in the  
113 soils.

114 The aims of this work were to: (i) determine Zn accumulation rates in grassland soils under  
115 current agricultural practices, (ii) differentiate between geogenic and anthropogenic Zn in the  
116 soils, and (iii) identify important Zn redistribution mechanisms in the soils.

117

## 118 **Materials and Methods**

### 119 *Study Sites*

120 The study was carried out at three grassland monitoring sites (Figure S1) of the Swiss Soil  
121 Monitoring Network (NABO)<sup>9</sup> at Tänikon (TA), Ebikon (EB), and Ependes (EP). The sites have  
122 been used as grasslands for at least the last 30 years and were chosen because of contrasting  
123 geology and soil properties. The soils developed on alluvial deposits (TA), sandstone (EB), and  
124 moraine material (EP). All three soils were classified as Eutric Cambisols. During the time of  
125 the field sampling, the sites were managed in the same way like in the years before our  
126 experiment. The grassland sites at TA and EB were cut 4 and 6 times during our study period,  
127 respectively, and the grassland site at EP was used for grazing of cows (Table S3). Liquid cow  
128 manure was applied at all sites, liquid pig manure was applied at TA and EB, and poultry dung  
129 was applied at EP every fourth year (Table S3).

### 130 *Sampling*

131 Soil samples were taken from five depths (0-10 cm, 10-20 cm, 20-50 cm, 50-75 cm, and >75  
132 cm, Figure S2). Inputs and outputs (Figure 1) were sampled during one hydrological year from  
133 May 2014 to May 2015. Soil parent material was collected at each site. The C horizons at TA  
134 (60-80 cm) and EP (120-140 cm) were obtained from the NABO<sup>9</sup> whereas sandstone at EB and  
135 moraine material at EP were sampled from nearby outcrops. Cumulative volumes of  
136 atmospheric deposition and seepage water were stored in canisters in the field and sampled  
137 every second week. The volumetric water content of the soils was determined with 1-h  
138 resolution by time domain reflectometry at 50 cm depth. Homogeneous liquid manure  
139 samples were taken four times a year at each site. During the growing season (2014.w28 to  
140 2014.w44 and 2105.w14 to 2015.w24), aboveground biomass was randomly sampled in  
141 triplicates at each site every fourth week.

### 142 *Laboratory Analysis*

143 Basic soil properties including pH, cation-exchange capacity (CEC), texture, bulk density,  
144 coarse soil content (> 2mm), and C, N, and S concentrations were analyzed and the soils were  
145 characterized according to the World Reference Base for Soil Resources (Table S1).<sup>57</sup>

146 Aliquots of seepage water samples were used to measure major cations ( $\text{Na}^+$ ,  $\text{NH}_4^+$ ,  $\text{K}^+$ ,  $\text{Mg}^{2+}$   
147 and  $\text{Ca}^{2+}$ ) and anions ( $\text{Cl}^-$ ,  $\text{NO}_2^-$ ,  $\text{NO}_3^-$ ,  $\text{PO}_4^{2-}$  and  $\text{SO}_4^{2-}$ ) by ion chromatography (IC, DX-120,  
148 ThermoFisher Scientific, Waltham, MA, USA). Accordingly, dissolved organic carbon (DOC)  
149 was measured with a vario TOC cube analyzer (Elementar Analysensysteme, Langenselbold,  
150 Germany). Total dissolved concentrations of the most abundant elements (Al, V, Mn, Fe, Co,  
151 Ni, Cu, Zn, As, Rb, Sr, Ba, and U) in atmospheric deposition and seepage water were measured  
152 by inductively-coupled mass spectrometry (ICP-MS, 7700x, Agilent Technology, Waldbronn,  
153 Germany) and used later for Zn speciation modeling.

154 The stable Zn isotope compositions of all samples were determined with standard-sample  
155 bracketing and Cu doping for instrumental mass-bias correction by multiple collector  
156 inductively-coupled plasma mass spectrometry (Neptune Plus™ High Resolution MC-ICP-MS,  
157 Thermo Fisher Scientific, Waltham, MA, USA) at the Geological Institute of the University of  
158 Bern (SI 1.3). The total procedural Zn blank for the isotope analysis of parent materials, soils,  
159 aboveground biomass, and manure samples (0.7 to 6.3 ng) accounted for less than 0.2% of  
160 the native Zn mass in the samples. The total procedural blanks of seepage water (71 to 75 ng)  
161 and bulk deposition (218 to 223 ng) accounted on average for 1.3% and 4.5% of the total Zn  
162 masses (SI 1.3). Several standard reference materials (SRMs) were analyzed for quality control  
163 (Table S2). The Zn isotope composition of ryegrass (BCR-CRM281) was slightly heavier than  
164 formerly reported values.<sup>47,58,59</sup> All other standards (USGS BCR-2 and CMI SCL7003) showed  
165 robust results in agreement with published values.<sup>60</sup>

166 The Zn stable isotope compositions of the samples were reported relative to the IRMM 3702  
167 Zn isotope reference material using a  $\delta$  notation based on the  $^{66}\text{Zn}/^{64}\text{Zn}$  ratio (Equation S1).  
168 The analytical error was 0.07‰, i.e. two times the standard deviation of the measured IRMM-  
169 3702 standards (n=11). Two samples were considered significantly different in their isotopic  
170 composition if their error bar (2 standard deviations of the repeated analysis of each sample)  
171 did not overlap. The  $\Delta^{66/64}\text{Zn}$  value, which denote the apparent isotopic fractionation between  
172 two reservoirs and/or two fluxes (e.g. between soil and seepage water) were calculated  
173 according to Equation S3.

174

## 175 *Modeling and Calculations*

176 Zn speciation in seepage water was calculated with Visual MINTEQ. The pH, cation, anion,  
177 total element, and dissolved organic matter (DOM) concentrations in soil solution were used  
178 as input data. Ionic strength was calculated by Visual MINTEQ. Dissolved organic matter  
179 concentrations were inferred from the measured dissolved organic C concentrations (DOC),  
180 using a conversion factor DOM:DOC of 2:1.<sup>61</sup> Zinc speciation was modelled with two  
181 scenarios, because it has been reported that the chemical DOM composition was an  
182 important source of uncertainty.<sup>62</sup> DOM in the min-HS (HS = humic substances) scenario  
183 consisted of 2% humic acids (HA), 18% fulvic acids (FA), and 80% hydrophilic organic  
184 substances and in the max-HS scenario of 6% humic acids, 54% fulvic acids and 40%  
185 hydrophilic organic substances, in line with reported values.<sup>62,63</sup>

186 Zinc and Ti concentrations in the parent materials and soils were used to calculate Zn mass  
187 gains or losses per unit volume of soils relative to parent materials ( $\tau_{Zn}$  values and remaining  
188 Zn fractions  $f_{Zn} = \tau_{Zn} + 1$ , SI 1.4).<sup>64</sup> Zn mass balances (SI 1.5) were calculated for each study soil  
189 in the upper soil layer (0-50 cm, Figure 1, Table S3), considering inputs from weathering,  
190 atmospheric deposition, and manure as well as outputs with seepage water, and  
191 aboveground biomass. Input from weathering was estimated as dissolution of the coarse soil  
192 (> 2mm) which introduced Zn to the fine earth.

193 We used three models to investigate the Zn (isotope) distribution in the soils, an  
194 *anthropogenic and atmospheric impact*, a *soil-plant cycling*, and a *Rayleigh fractionation*  
195 model for soil formation. The outputs of the models were described in **Cases A, B, and C** for  
196 which  $f_{Zn}$  and  $\delta^{66}Zn$  values of the soils were calculated. Overall, a combination of the models  
197 was used to explain the depth distribution of the Zn concentrations and stable isotope ratios  
198 in the soils. **Case A** was the starting point of the model calculations, using current values in the  
199 year 2015 including anthropogenic impacts, atmospheric deposition, and soil-plant cycling.  
200 From there, the *anthropogenic and atmospheric impact model* was used to assess the  
201 importance of anthropogenic and atmospheric fluxes for the Zn stocks and Zn isotope  
202 compositions of the soils (SI 1.6). These calculations were based on measured Zn fluxes and  
203 isotope compositions as well as on literature data on past manure inputs and atmospheric

204 deposition.<sup>10,12</sup> The output of this model was **Case B**, describing the state in the year 1915  
 205 without anthropogenic impact and atmospheric deposition. To arrive at this case, estimated  
 206 past outputs were added and estimated past inputs subtracted from the current bulk soil Zn  
 207 stocks (Equation S8) and bulk soil isotope compositions (Equation S9). Next, the *soil-plant*  
 208 *cycling model*<sup>54</sup> was used to investigate if trees, the potential native vegetation which  
 209 formerly covered the agricultural soils, took up Zn from the deeper soil horizons and added it  
 210 to the upper soil horizons, over the time of soil formation. Thereby, the soils were first  
 211 subdivided into two layers (0-39 cm and 39-78 cm). For these two layers, we derived the  
 212 remaining Zn fractions ( $f_{Zn} = \tau_{Zn} + 1$ ) and the  $\delta^{66}Zn$  values by averaging the respective values of  
 213 five bulk soil layers 0-10 cm, 10-20 cm, 20-50 cm, 50-75 cm, >75 cm from **Case B**.  
 214 Furthermore, the potential Zn surplus in the upper (0-39 cm) relative to the deeper (39-78  
 215 cm) soil layer, presumably cycled by trees,<sup>54</sup> was calculated with the help of  $\tau_{Zn}$  values. This  
 216 potential Zn surplus was divided by the age of the soils (13,600 years in 1915)<sup>65-67</sup> to obtain  
 217 the annually cycled Zn. Next, the annually cycled Zn mass was subtracted from the upper and  
 218 added to the deeper soil-layer, in 13,600 steps to incrementally reverse the assumed process  
 219 during the soil formation before the start of intensified agriculture. Additionally, the change in  
 220 Zn isotope composition of the two soil layers was calculated (Equations S10 and S11) by  
 221 subtracting the Zn isotope composition of the annually cycled Zn from the upper and adding it  
 222 to the deeper soil-layer in the same 13,600 annual steps. The isotope composition of the  
 223 cycled Zn was determined for each calculation step using the measured  $\Delta^{66}Zn_{soil-aboveground}$   
 224  $_{biomass}$  values at the three study sites (SI 1.7). After 13,600 calculation steps, the  $f_{Zn}$  and  $\delta^{66}Zn$   
 225 values were averaged for the two soil-layers and represented **Case C**, i.e. the state in the year  
 226 1915 without anthropogenic and atmospheric impact and without soil-plant cycling. Error  
 227 propagation was calculated according to Imseng et al.<sup>54</sup> Finally, the  $f_{Zn}$  and  $\delta^{66}Zn$  values of  
 228 **Case C** were used in a *Rayleigh fractionation model* to describe the soil isotope composition  
 229 change during parent material weathering and Zn leaching with seepage water (Equation 1).

230 *Equation 1:*  $\Delta^{66}Zn_{soil-parent\ material} = \varepsilon \ln f_{Zn}$

231 where  $\Delta^{66}Zn_{soil-parent\ material}$  is the difference in the  $\delta^{66}Zn$  value between a soil layer and its  
 232 parent material and  $\varepsilon$  is the Rayleigh fractionation factor for soil formation.

233

## 234 Results

235 Our mass balances revealed that the current Zn inputs were 2 to 4 times higher than Zn  
236 outputs. Consequently, the Zn mass balances showed net accumulations at all three sites,  
237 which were the highest at TA (1,476 g ha<sup>-1</sup> yr<sup>-1</sup>) followed by EB (1,070 g ha<sup>-1</sup> yr<sup>-1</sup>) and EP (456 g  
238 ha<sup>-1</sup> yr<sup>-1</sup>, Figure 1, Table S3). The quantitatively most important Zn input was manure  
239 application (1,078 to 1,857 g ha<sup>-1</sup> yr<sup>-1</sup>) which accounted for more than 98% of the total Zn  
240 inputs at all three sites. In contrast, Zn inputs from atmospheric deposition (20 to 39 g ha<sup>-1</sup> yr<sup>-1</sup>)  
241 and weathering (0.01 to 8.6 g ha<sup>-1</sup> yr<sup>-1</sup>) were considerably smaller. Outputs with  
242 aboveground biomass (315, 312 and 585 g ha<sup>-1</sup> yr<sup>-1</sup>) exceeded outputs with seepage water  
243 (99, 16 and 55 g ha<sup>-1</sup> yr<sup>-1</sup>) at TA, EB and EP, respectively.

244 Parent material isotope compositions ranged from -0.07‰ to 0.07‰ at the three sites (Figure  
245 S3, Table S3). The soil at TA was on average isotopically slightly heavier ( $\Delta^{66}\text{Zn}_{\text{soil}(0-75\text{cm})\text{-C horizon}} = 0.07 \pm 0.07\text{‰}$ ) and the soil at EB ( $\Delta^{66}\text{Zn}_{\text{soil}(0-75\text{cm})\text{-sandstone}} = -0.11 \pm 0.07\text{‰}$ ) isotopically lighter  
247 than the parent materials. In contrast, the soil at EP ( $\Delta^{66}\text{Zn}_{\text{soil}(0-75\text{cm})\text{-parent materials}} = 0.00$   
248  $\pm 0.07\text{‰}$ ) was on average isotopically not different from the parent materials. The Zn isotopic  
249 compositions of the inputs and outputs were on average little different from the soils or  
250 isotopically lighter (Figure S3, Table S3). First, the manure was more enriched in light Zn  
251 isotopes than the soil at TA ( $\Delta^{66}\text{Zn}_{\text{soil}(0-75\text{cm})\text{-manure}} = 0.14 \pm 0.07\text{‰}$ ), but slightly more enriched in  
252 heavy isotopes than the soils at EB ( $-0.06 \pm 0.07\text{‰}$ ) and EP ( $-0.05 \pm 0.07\text{‰}$ ). Second, the  
253 atmospheric deposition was on average more enriched in light Zn isotopes than the soils at TA  
254 ( $\Delta^{66}\text{Zn}_{\text{soil}(0-75\text{cm})\text{-atm. dep.}} = 0.32 \pm 0.03\text{‰}$ ), EB ( $0.23 \pm 0.07\text{‰}$ ), and EP ( $0.13 \pm 0.07\text{‰}$ ). Third,  
255 compared with the soils, seepage water was on average Zn-isotopically lighter at TA  
256 ( $\Delta^{66}\text{Zn}_{\text{soil}(0-75\text{cm})\text{-seepage water}} = 0.59 \pm 0.05\text{‰}$ ) but Zn-isotopically heavier at EB ( $-0.11 \pm 0.07\text{‰}$ ) and  
257 EP ( $-0.10 \pm 0.07\text{‰}$ ). Finally, the aboveground biomass was slightly more enriched in light Zn  
258 isotopes than the soil at TA ( $\Delta^{66}\text{Zn}_{\text{soil}(0-75\text{cm})\text{-aboveground biomass}} = 0.09 \pm 0.07\text{‰}$ ) and Zn-isotopically  
259 identical to the soil at EB ( $0.00 \pm 0.07\text{‰}$ ) and EP ( $-0.06 \pm 0.07\text{‰}$ ).

260

## 261 Discussion

262 *Zn Mass Balances*

263 *Input Fluxes.* The size of the Zn input with manure was related to the type of manure, because  
264 Zn concentrations in pig manure (384 to 962 mg Zn kg dry weight<sup>-1</sup>) were higher than Zn  
265 concentrations in cow manure (133 to 311 mg Zn kg dry weight<sup>-1</sup>). The proportion of pig  
266 manure of the total addition of manure (dry weight, Table S3) was bigger at TA (19%) than at  
267 EB (6%) whereas only cow manure and poultry dung were spread at EP. Therefore, Zn input  
268 with manure was highest at TA, followed by EB and EP (Figure 1). The Zn inputs with manure  
269 in our study fell into the range of reported values for European agricultural soils (300 to 2,700  
270 g ha<sup>-1</sup> yr<sup>-1</sup>).<sup>10-12</sup> Atmospheric deposition of Zn was by one to two orders of magnitude smaller  
271 than Zn inputs with manure and varied only by a factor of two among the sites (19.5 to 38.8 g  
272 ha<sup>-1</sup> yr<sup>-1</sup>). The deposition rates were below reported values for Swiss agricultural soils in 2003  
273 (80 to 130 g ha<sup>-1</sup> yr<sup>-1</sup>)<sup>10</sup> and in the lower range of atmospheric deposition rates for European  
274 soils (20 to 540 g ha<sup>-1</sup> yr<sup>-1</sup>).<sup>20</sup> The low deposition rates of Zn in our study might be related to  
275 the rural location of our sites and the recently decreasing anthropogenic Zn emissions to the  
276 atmosphere.<sup>17,18,68</sup> Zinc input from weathering was the highest at TA (0.5% of the total Zn  
277 inputs) and negligible at EB and EP. The comparatively high contribution of Zn from  
278 weathering at TA can be attributed to the calcareous coarse soil for which reported  
279 weathering rates<sup>69</sup> are three orders of magnitude higher than for the silicatic coarse soils<sup>70,71</sup>  
280 at the two other sites.

281 *Output Fluxes.* Despite similar amounts of harvested biomass among the sites, Zn output with  
282 aboveground biomass was about 1.6 times higher at EP than at TA and EB, mainly because of  
283 the higher average Zn concentrations in aboveground biomass at EP (Table S3). The Zn  
284 concentrations in aboveground biomass and Zn outputs with aboveground biomass were in  
285 the range of recently reported values.<sup>10,22,72</sup> The decreasing Zn outputs with seepage water  
286 from TA via EB to EP can be explained by the declining Zn concentrations (Table S2). Our  
287 results are at the lower end of reported leaching rates for European soils (18 and 135 g ha<sup>-1</sup>  
288 yr<sup>-1</sup>).<sup>11,12,22,23</sup>

289 *Balance.* The most influential driver for the Zn mass balance of the soils was manure  
290 application,<sup>73</sup> causing a considerable net accumulation of Zn in all three soils. The predicted  
291 accumulation agrees well with recently reported trends for Zn accumulation on intensively  
292 used grassland soils.<sup>9</sup>

293

## 294 *Origin of the Zn in the Soils*

295 The Zn distribution in the grassland soils is a result of different Zn inputs (manure,  
296 weathering, and atmospheric deposition), Zn outputs (aboveground biomass, seepage water),  
297 and soil formation processes. To better understand the origin of the Zn in the soils, the Zn  
298 isotope fluxes are discussed in a first step. Subsequently, the stable Zn isotopes were used in  
299 our *anthropogenic and atmospheric impact model*, to assess the importance of anthropogenic  
300 inputs for the Zn distribution in the soils.

301 *Zn isotope fluxes.* The isotopic composition of parent materials (Figure S3, Table S3) was in the  
302 range of formerly measured values for crustal rocks and minerals (-0.22 to 0.28‰).<sup>74,75</sup>  
303 Furthermore, the soils showed only little Zn-isotopic differences (at most 0.13‰ lighter or  
304 0.10‰ heavier) from the parent materials. This indicates, that weathering only marginally  
305 influenced Zn-isotopic compositions of the soils, even though between 12% and 58% (except  
306 0-10 cm at EB) of the initial Zn was lost from the soils (revealed by  $\tau_{Zn}$  values), probably mainly  
307 with seepage water. Similarly, a study on Zn isotope fractionation during soil development  
308 found on average small differences in stable Zn isotope ratios between parent material and  
309 soil ( $\Delta^{66}Zn_{\text{parent material-soil}} \leq 0.20\text{‰}$ ) at Zn losses between 0 and 95% suggesting a generally weak  
310 influence of soil formation on Zn isotopic compositions.<sup>34</sup>

311 The average isotopic composition of manure was similar to the isotopic composition of the  
312 aboveground biomass. One reason for this could be that Zn in feed additives was isotopically  
313 little different from Zn in the aboveground biomass and that digestion in the farmland animal  
314 digestive tract caused only minor isotopic fractionation. Alternatively, digestive processes  
315 might have caused isotopic fractionations but were counterbalanced by an isotopic signature  
316 of the feed additives which deviated from that in the basic feed in the opposite direction than  
317 this fractionation. Isotopic compositions of recently analyzed pig slurries (-0.11 and -  
318 0.08‰)<sup>30</sup> were slightly lighter than or identical to our values.

319 The similar isotopic compositions of the atmospheric deposition among the three sites  
320 indicate similar Zn sources or sources with similar  $\delta^{66}Zn$  values. This Zn might partly derive  
321 from natural sources because its isotope composition is in the range of rural rain water  
322 samples (-0.32 to -0.17‰),<sup>76</sup> igneous rocks and minerals (-0.22 to 0.28‰),<sup>30,74,75</sup> aboveground  
323 plant material (-0.50 to 0.50‰),<sup>25</sup> and aerosols from the North Atlantic (-0.29 to -0.15‰).<sup>77</sup>

324 Alternatively, the Zn could also originate from anthropogenic sources, because bus air filters  
325 in urban areas (-0.22 to -0.28‰) and waste incineration flue gas samples (-0.25 to -0.13‰)  
326 showed similar isotopic compositions.<sup>78</sup> In contrast, smelting processes and gasoline  
327 combustion seemed to be of less importance at our sites as dust from smelter chimneys (-  
328 0.99 to -0.95‰)<sup>26,27</sup> and aerosols from urban areas (-1.41 to -0.41‰)<sup>79</sup> were isotopically  
329 lighter.

330 The isotope fractionation between soil and seepage water was different among the three  
331 sites. At TA, the site with the highest pH and ionic strength, Zn in seepage water was much  
332 lighter than at EB and EP, the sites with lower pH and ionic strength. Several studies  
333 investigated the isotopic fractionation during Zn adsorption to quartz and amorphous SiO<sub>2</sub>,<sup>37</sup>  
334 kaolinite,<sup>39</sup> (hydr)oxides,<sup>35,36,80</sup> organic matter,<sup>40</sup> and calcite<sup>38</sup> and found stronger enrichments  
335 of heavier isotopes with increasing specificity of the bonds (inner-sphere vs. outer-sphere;  
336 high-affinity vs. low affinity; tetrahedral vs. octahedral). This can be explained by the bond  
337 lengths of Zn with its neighboring atoms, which become shorter with increasing  
338 specificity.<sup>35,37</sup> Thereby, increasing pH and ionic strength drove the Zn to bind to more specific  
339 adsorption sites and hence led to stronger enrichments of heavy isotopes at the surfaces  
340 while leaving the solutions isotopically lighter.<sup>35-38,40</sup> In our study, the higher pH at TA than at  
341 EP and EB might have favored a more pronounced specific binding of Zn and caused the  
342 depletion of heavy Zn in the seepage water at TA. Furthermore, the higher Mg<sup>2+</sup> and Ca<sup>2+</sup>  
343 concentrations in soil solutions at TA (18 ±4 mg L<sup>-1</sup> and 77 ±19 mg L<sup>-1</sup>) than at EB (2.3 ±0.4 mg  
344 L<sup>-1</sup> and 17 ±3 mg L<sup>-1</sup>) and EP (1.5 ±0.4 mg L<sup>-1</sup> and 24 ±6 mg L<sup>-1</sup>) might have been important  
345 competitors of Zn for the less specific binding sites at the mineral surfaces in soil. As a  
346 consequence, the preferential binding of isotopically heavy Zn to the more specific binding  
347 sites might have been further enhanced. This hypothesis is supported by the Zn speciation  
348 modeling, which showed that between 61% (max-HS scenario) and 90% (min-HS scenario,  
349 Table S4) of the dissolved Zn was present as free Zn<sup>2+</sup> and only a minor part complexed by  
350 organic acids while other Zn species only occurred in negligible concentrations. Hence, the  
351 potential enrichment of isotopically heavy Zn in Zn-DOM complexes seems to be only of  
352 minor importance at our sites.

353 The stronger enrichment of light isotopes in the aboveground biomass than in the soil at TA  
354 might be a consequence of the isotopically light Zn in soil solution, from where plants take up

355 their nutrients. In contrast, at EB and EP, the sites with a Zn-isotopically slightly heavier soil  
356 solution than bulk soil, no isotopic difference was measured between aboveground biomass  
357 and bulk soil. Several studies investigated Zn uptake and translocation mechanisms with the  
358 help of Zn stable isotopes. Thereby, low affinity uptake, which is expected to dominate at Zn  
359 concentrations above 10 nmol L<sup>-1</sup> (like at our sites),<sup>81</sup> was associated with no isotopic  
360 fractionation or the preferential uptake of light isotopes.<sup>32,44,82,83</sup> Furthermore, Zn  
361 translocation in plants was linked with the preferential retention of heavy isotopes in roots  
362 and transport of light isotopes to aboveground plant tissues.<sup>32,84</sup> At our sites, aboveground  
363 biomass was isotopically not distinct or heavier than seepage water. This might be a  
364 consequence of the purposeful acidification of the rhizosphere soil by the plants to mobilize  
365 nutrients, particularly phosphorus. As side effect, also micronutrients like Zn were mobilized  
366 and rendered the plant-available Zn isotopically heavier, like it was reported for *Agrostis*  
367 *capillaris* L. on Zn-contaminated soils.<sup>41</sup> This effect was strongest at TA, the site with the  
368 highest pH and highest  $\Delta^{66}\text{Zn}_{\text{soil-seepage water}}$  value.

369 *Anthropogenic and atmospheric impact on the Zn in soils.* To be able to investigate natural Zn  
370 redistribution processes in soils, former anthropogenic and atmospheric impacts on the soil  
371 Zn concentrations were mathematically removed with the *anthropogenic and atmospheric*  
372 *impact model*. For that model, we simplified our agricultural systems and assumed that they  
373 were only anthropogenically influenced during the last 100 years, which is justified by two  
374 reasons. First, Zn concentrations in Alpine snow and ice core samples correlated with  
375 anthropogenic Zn emissions and indicated that atmospheric deposition rates were 30 times  
376 lower during the 18<sup>th</sup> and 19<sup>th</sup> centuries than in the 1970s.<sup>18,19</sup> Further, even in the 18<sup>th</sup> and  
377 19<sup>th</sup> century, only 14% of the deposited Zn was of natural origin. Thus, atmospheric  
378 deposition rates before the industrialization can be expected to be 200fold lower than in the  
379 1970s, i.e.  $\sim 1 \text{ g ha}^{-1} \text{ yr}^{-1}$ . Second, feed additives and Zn input with manure became more  
380 important after World War I, with intensification of agricultural practices and the use of  
381 concentrated animal food.<sup>3,4</sup> Before that time, annual Zn fluxes with fertilization and harvest  
382 were considerably smaller than during the 20<sup>th</sup> century. Therefore, in our study, soils were  
383 considered as closed systems regarding the Zn fluxes.<sup>3</sup>

384 For the further investigations of natural soil formation processes, the soils were subdivided  
385 into two layers (0-39 cm and 39-78 cm) and  $\tau_{\text{Zn}}$  as well as Zn isotope compositions were

386 averaged for both layers. In that way, also the influence of anthropogenic activities and  
387 former atmospheric deposition could be estimated for these two soil layers. For **Case A**  
388 (referring to the year 2015), the remaining Zn fractions ( $f_{Zn}$ ) were higher in the upper (0-39  
389 cm) than in the deeper (39-78 cm) soil layers (Figures 2, 3a, S4, S5). This Zn distribution was  
390 partly caused by anthropogenic inputs and historic atmospheric inputs. According to our  
391 model calculations, anthropogenic impacts (16%, 18% and 6%) and historic atmospheric  
392 deposition (4%, 4% and 4%) increased the Zn stocks in the upper soil layer (0-39 cm) at TA, EB  
393 and EP, respectively. For the deeper soil layer (39-78 cm), these increases were considerably  
394 smaller at all three sites accounting for only 2% of the stocks. However, even without  
395 anthropogenic impact and former atmospheric deposition (**Case B** referring to the year 1915),  
396  $f_{Zn}$  values are higher in the upper (0-39 cm) than in the deeper soil layer (39-78 cm), which  
397 will be discussed in the next chapter. As outlined above, the Zn stocks and Zn isotopic  
398 compositions were only marginally influenced by humans before 1915. Furthermore, the  
399 historic atmospheric inputs have been considered and subtracted. For these reasons, **Case B**  
400 can be used to further investigate Zn redistribution processes in soils.

401

#### 402 *Zn Redistribution Processes in the Soils*

403 As mentioned above, even without anthropogenic impact and former atmospheric inputs  
404 (**Case B**), remaining Zn fractions ( $f_{Zn}$ ) were higher in the upper (0-39 cm) than in the deeper  
405 (39-78 cm) soil layers (Figures 2, S4, S5, 3b, 3c). However, if leaching with seepage water was  
406 the only important process during soil formation we would expect the upper older soil  
407 horizons to be more depleted in Zn than the younger deeper soil horizons. Several studies  
408 revealed the importance of the plant pump for the distribution of nutrients<sup>55,56</sup> and metals in  
409 soils.<sup>54,85-87</sup> Here, we applied a soil-plant cycling model<sup>54</sup> to assess the importance of the plant  
410 pump for the Zn distribution in the studied soils. After removal of the soil-plant cycling effect  
411 (**Case C**), the remaining Zn fractions were smaller in the upper than in the deeper soil-layer  
412 (Figures 2, S4, S5, 3d). Furthermore, by subtracting the influence of soil-plant cycling, it was  
413 possible to fit Rayleigh-type fractionation models between soil solid phase and soil solution  
414 for the three soils. These models resulted in different apparent fractionation factors during  
415 weathering and soil formation ( $\epsilon$ ) of -0.18, 0.18 and 0.00 at TA, EB and EP, respectively (Figure

416 3d), suggesting that different pedogenetic Zn-fractionation processes were at play at the  
417 three study sites. The finding that the Zn isotope fractionation derived from the Rayleigh-type  
418 model differed among the study sites deviated from our previously reported similarly derived  
419 finding for Cd.<sup>54</sup> In contrast to Zn, the Cd isotope fractionation between solid soil and seepage  
420 water was constant among the sites, despite differing soil pH values.<sup>88</sup> For Zn, the different  
421 directions of the isotope fractionation coincided with different soil pH values at the three  
422 sites (Figure 3e). While these patterns can be interpreted independently for the three  
423 different soils, which formed from different parent materials, it can also be assumed that the  
424 three soils follow one overall pattern controlling the Zn isotope fractionation in soils  
425 depending on the pH. Hypothesizing one overall pattern, the sequence might start at TA and  
426 end at EB. With the presence of carbonates and an alkaline soil pH like at TA, isotopically light  
427 Zn was leached with seepage water and shifted the isotope composition of the soil towards  
428 heavier values. With the depletion of the carbonate buffer and a slightly acidic soil pH like at  
429 EP, isotopically heavy Zn was leached from the soil and shifted its isotope composition toward  
430 lighter values thereby compensation the previous fractionation in the other direction, which  
431 might explain the isotopic similarity of Zn in bulk soil and parent material. With ongoing soil  
432 acidification like at EB, heavy Zn isotopes were continuously leached and caused the bulk soil  
433 to be isotopically lighter than the parent material. However, our hypothesis of this overall  
434 pattern would need further confirmation from additional soils.

435

### 436 *Environmental Implications*

437 The most influential driver for the Zn mass balance of the soils was manure application.<sup>73</sup> The  
438 current Zn concentrations in the topsoils (85 to 122 mg kg<sup>-1</sup>, Table S1) might already be toxic  
439 for some plants,<sup>89</sup> invertebrates,<sup>90</sup> and microorganisms.<sup>91</sup> If current agricultural practices  
440 continue in the future, soil Zn concentrations will further increase. Assuming the same Zn  
441 addition of inputs and Zn removal of outputs from the different soil layers like in the  
442 anthropogenic and atmospheric impact model (SI 1.6), the largest part of Zn would remain in  
443 the uppermost soil layer (0-20 cm) and the Zn stock of this horizon would increase by 68%,  
444 36% and 22% within 100 years at TA, EB and EP, respectively. This represents a faster  
445 accumulation than in the last 100 years. Between 1915 and 2015, the Zn stocks in the

446 uppermost soil layer (0-20 cm) increased only by 30%, 26% and 8% at TA, EB and EP,  
447 respectively, because of the lower Zn inputs with manure. Over the millennia of soil  
448 development, soil-plant cycling, mineral weathering, and leaching were more relevant than  
449 the anthropogenic Zn inputs of the past few decades. However, under the current agricultural  
450 practice the anthropogenic impact will probably overprint the natural Zn distribution in soils,  
451 causing possible harmful Zn concentrations in the surface soils. The predicted accumulation  
452 supports recently reported trends for Zn accumulation on intensively used grassland soils.<sup>9</sup> To  
453 prevent further Zn accumulation in soils, it is crucial that Zn in feed additives for farm animals  
454 are not above the required doses and that the quantity of manure applied to a specific area is  
455 limited. According the European Food Safety Authority (EFSA), the authorized maximum Zn  
456 concentrations in animal feed could be reduced by 20% without compromising health,  
457 welfare, and productivity of the target animals.<sup>72</sup> Furthermore, the use of phytase could  
458 enhance the Zn availability for non-ruminants and allow for a reduction of even 30% of the  
459 currently authorized maximum concentrations for pigs.<sup>72</sup>

460

## 461 **Supporting information**

462 Section 1: Detailed information on materials and methods. Section 2: Location of the study  
463 sites. Section 3: Sampling design. Section 4: Isotope compositions of all measured samples.  
464 Section 5: Soil-plant cycling models for TA and EP. Section 6: Soil properties. Section 7:  
465 Standard reference materials. Section 8: Zn mass balance and anthropogenic impact model.  
466 Section 9: Seepage water properties.

467

## 468 **Acknowledgements**

469 This study was funded by the Swiss Parliament via the National Research Program (NRP) 69  
470 “Healthy Nutrition and Sustainable Food Production” (SNSF grant no. 406940\_145195/1). We  
471 thank the farmers from the study sites for cooperation, Lise Missiaen and Claudia Loretz for  
472 the characterization of the soils and Martin Wille for the help with isotope measurements.  
473 Many thanks to the members of the Soil Science and TrES groups at the University of Bern for  
474 support in the laboratory and helpful discussions.

## 475 References

- 476 (1) Sheppard, S. C.; Sanipelli, B. Trace Elements in Feed, Manure, and Manured Soils. *J.*  
477 *Environ. Qual.* **2012**, *41* (6), 1846 DOI: 10.2134/jeq2012.0133.
- 478 (2) Wilcke, W.; Döhler, H. *Schwermetalle in der Landwirtschaft: Quellen, Flüsse, Verbleib*;  
479 Darmstadt, 1995.
- 480 (3) Frossard, E.; Bünemann, E.; Jansa, J.; Oberson, A.; Feller, C. Concepts and practices of  
481 nutrient management in agro-ecosystems: Can we draw lessons from history to design  
482 future sustainable agricultural production systems? *Die Bodenkultur* **2009**, No. 60(1),  
483 43–60.
- 484 (4) Spiess, E. Nitrogen, phosphorus and potassium balances and cycles of Swiss agriculture  
485 from 1975 to 2008. *Nutr. Cycl. Agroecosystems* **2011**, *91* (3), 351–365.
- 486 (5) Mantovi, P.; Bonazzi, G.; Maestri, E.; Marmioli, N. Accumulation of copper and zinc  
487 from liquid manure in agricultural soils and crop plants. *Plant Soil* **2003**, *250* (2), 249–  
488 257 DOI: 10.1023/A:1022848131043.
- 489 (6) Bolan, N. S.; Adriano, D. C.; Mahimairaja, S. Distribution and bioavailability of trace  
490 elements in livestock and poultry manure by-products. *Critical Reviews in*  
491 *Environmental Science and Technology*. May 2004, pp 291–338.
- 492 (7) Gräber, I.; Hansen, J. F.; Olesen, S. E.; Petersen, J.; Øtergaard, H. S.; Krogh, L.  
493 Accumulation of copper and zinc in Danish agricultural soils in intensive pig production  
494 areas. *Geogr. Tidsskr.* **2005**, *105* (2), 15–22 DOI: 10.1080/00167223.2005.10649536.
- 495 (8) Xue, H.; Sigg, L.; Gächter, R. Transport of Cu, Zn and Cd in a small agricultural  
496 catchment. *Water Res.* **2000**, *34* (9), 2558–2568 DOI: 10.1016/S0043-1354(00)00015-4.
- 497 (9) Gubler, A.; Schwab, P.; Wächter, D.; Meuli, R. G.; Keller, A. *Ergebnisse der Nationalen*  
498 *Bodenbeobachtung (NABO) 1985-2009*; 2015.
- 499 (10) Keller, A.; Rossier, N.; Desaulles, A. *Schwermetallbilanzen von Landwirtschaftsparzellen*  
500 *der nationalen Bodenbeobachtung: NABO - Nationales Bodenbeobachtungsnetz der*  
501 *Schweiz*; Schriftenreihe der FAL; FAL: Zürich, 2005; Vol. 54.

- 502 (11) Bengtsson, H.; Öborn, I.; Jonsson, S.; Nilsson, I.; Andersson, A. Field balances of some  
503 mineral nutrients and trace elements in organic and conventional dairy farming - A  
504 case study at Öjebyn, Sweden. In *European Journal of Agronomy*; 2003; Vol. 20, pp  
505 101–116.
- 506 (12) Keller, A.; Schulin, R. Modelling regional-scale mass balances of phosphorus, cadmium  
507 and zinc fluxes on arable and dairy farms. *Eur. J. Agron.* **2003**, *20* (1–2), 181–198 DOI:  
508 10.1016/S1161-0301(03)00075-3.
- 509 (13) European Union. *Risk Assessment Report. Zinc Metal. Part I - Environment.*; Publications  
510 Office of the European Union, 2010.
- 511 (14) He, Z. L.; Yang, X. E.; Stoffella, P. J. Trace elements in agroecosystems and impacts on  
512 the environment. *J. Trace Elem. Med. Biol.* **2005**, *19* (2–3), 125–140 DOI:  
513 10.1016/j.jtemb.2005.02.010.
- 514 (15) Mertens, J.; Smolders, E. Zinc: In: Heavy Metals in Soils: Trace Metals and Metalloids in  
515 Soils and their Bioavailability. In *Heavy Metals in Soils*; Springer, Dordrecht, 2013; Vol.  
516 22, pp 465–493.
- 517 (16) Nriagu, J. O. A global assessment of natural sources of atmospheric trace metals.  
518 *Nature* **1989**, *338* (6210), 47–49 DOI: 10.1038/338047a0.
- 519 (17) Nriagu, J. O.; Pacyna, J. M. Quantitative assessment of worldwide contamination of air,  
520 water and soils by trace metals. *Nature* **1988**, *333* (6169), 134–139 DOI:  
521 10.1038/333134a0.
- 522 (18) Olendzynski, K.; Anderberg, S.; Bartnicki, J.; Pacyna, J. M.; Stigliani, W. *Atmospheric*  
523 *emissions and deposition of cadmium, lead and zinc in Europe during the period 1955-*  
524 *1987*; WP-95-35; Laxenburg, 1995.
- 525 (19) Van de Velde, K.; Boutron, C. F.; Ferrari, C. P.; Moreau, A.-L.; Delmas, R. J.; Barbante, C.;  
526 Bellomi, T.; Capodaglio, G.; Cescon, P. A two hundred years record of atmospheric  
527 cadmium, copper and zinc concentrations in high altitude snow and ice from the  
528 French-Italian Alps. *Geophys. Res. Lett.* **2000**, *27* (2), 249 DOI: 10.1029/1999GL010786.
- 529 (20) Nicholson, F. A.; Smith, S. R.; Alloway, B. J.; Carlton-Smith, C.; Chambers, B. J. An

- 530 inventory of heavy metals inputs to agricultural soils in England and Wales. *Sci. Total*  
531 *Environ.* **2003**, *311* (1–3), 205–219 DOI: 10.1016/S0048-9697(03)00139-6.
- 532 (21) Degryse, F.; Smolders, E.; Parker, D. R. Partitioning of metals (Cd, Co, Cu, Ni, Pb, Zn) in  
533 soils: concepts, methodologies, prediction and applications - a review. *Eur. J. Soil Sci.*  
534 **2009**, *60* (4), 590–612 DOI: 10.1111/j.1365-2389.2009.01142.x.
- 535 (22) Moolenaar, S.; Lexmond, T. Heavy-metal balances of agro-ecosystems in the  
536 Netherlands. *Netherlands J. Agric. Sci.* **1998**, No. 46, 171–192.
- 537 (23) Fernandez, A.; Borrok, D. M. Fractionation of Cu, Fe, and Zn isotopes during the  
538 oxidative weathering of sulfide-rich rocks. *Chem. Geol.* **2009**, *264* (1–4), 1–12 DOI:  
539 10.1016/j.chemgeo.2009.01.024.
- 540 (24) Wiederhold, J. G. Metal Stable Isotope Signatures as Tracers in Environmental  
541 Geochemistry. *Environ. Sci. Technol.* **2015**, *49* (5), 2606–2624 DOI: 10.1021/es504683e.
- 542 (25) Moynier, F.; Vance, D.; Fujii, T.; Savage, P. The Isotope Geochemistry of Zinc and  
543 Copper. *Rev. Mineral. Geochemistry* **2017**, *82* (1), 543–600 DOI:  
544 10.2138/rmg.2017.82.13.
- 545 (26) Mattielli, N.; Petit, J. C. J.; Deboudt, K.; Flament, P.; Perdrix, E.; Taillez, A.; Rimetz-  
546 Planchon, J.; Weis, D. Zn isotope study of atmospheric emissions and dry depositions  
547 within a 5 km radius of a Pb-Zn refinery. *Atmos. Environ.* **2009**, *43* (6), 1265–1272 DOI:  
548 10.1016/j.atmosenv.2008.11.030.
- 549 (27) Sonke, J. E.; Sivry, Y.; Viers, J.; Freydier, R.; Dejonghe, L.; André, L.; Aggarwal, J. K.;  
550 Fontan, F.; Dupré, B. Historical variations in the isotopic composition of atmospheric  
551 zinc deposition from a zinc smelter. *Chem. Geol.* **2008**, *252* (3–4), 145–157 DOI:  
552 10.1016/j.chemgeo.2008.02.006.
- 553 (28) Yin, N. H.; Sivry, Y.; Benedetti, M. F.; Lens, P. N. L.; van Hullebusch, E. D. Application of  
554 Zn isotopes in environmental impact assessment of Zn-Pb metallurgical industries: A  
555 mini review. *Appl. Geochemistry* **2015**, *64*, 128–135 DOI:  
556 10.1016/j.apgeochem.2015.09.016.
- 557 (29) Bigalke, M.; Kersten, M.; Weyer, S.; Wilcke, W. Isotopes Trace Biogeochemistry and

- 558 Sources of Cu and Zn in an intertidal soil. *Soil Sci. Soc. Am. J.* **2013**, 77 (2), 680–691 DOI:  
559 DOI 10.2136/sssaj2012.0225.
- 560 (30) Fekiacova, Z.; Cornu, S.; Pichat, S. Tracing contamination sources in soils with Cu and Zn  
561 isotopic ratios. *Sci. Total Environ.* **2015**, 517, 96–105 DOI:  
562 10.1016/j.scitotenv.2015.02.046.
- 563 (31) Albarede, F. The Stable Isotope Geochemistry of Copper and Zinc. *Rev. Mineral.*  
564 *Geochemistry* **2004**, 55 (1), 409–427 DOI: 10.2138/gsrmg.55.1.409.
- 565 (32) Caldelas, C.; Weiss, D. J. Zinc Homeostasis and isotopic fractionation in plants: a review.  
566 *Plant Soil* **2017**, 411 (1–2), 17–46 DOI: 10.1007/s11104-016-3146-0.
- 567 (33) Weiss, D. J.; Boye, K.; Caldelas, C.; Fendorf, S. Zinc Isotope Fractionation during Early  
568 Dissolution of Biotite Granite. *Soil Sci. Soc. Am. J.* **2014**, 78 (1), 171 DOI:  
569 10.2136/sssaj2012.0426.
- 570 (34) Vance, D.; Matthews, A.; Keech, A.; Archer, C.; Hudson, G.; Pett-Ridge, J.; Chadwick, O.  
571 A. The behaviour of Cu and Zn isotopes during soil development: Controls on the  
572 dissolved load of rivers. *Chem. Geol.* **2016**, 445, 36–53 DOI:  
573 10.1016/j.chemgeo.2016.06.002.
- 574 (35) Juillot, F.; Maréchal, C.; Ponthieu, M.; Cacaly, S.; Morin, G.; Benedetti, M.; Hazemann, J.  
575 L.; Proux, O.; Guyot, F. Zn isotopic fractionation caused by sorption on goethite and 2-  
576 Lines ferrihydrite. *Geochim. Cosmochim. Acta* **2008**, 72 (19), 4886–4900 DOI:  
577 10.1016/j.gca.2008.07.007.
- 578 (36) Balistrieri, L. S.; Borrok, D. M.; Wanty, R. B.; Ridley, W. I. Fractionation of Cu and Zn  
579 isotopes during adsorption onto amorphous Fe(III) oxyhydroxide: Experimental mixing  
580 of acid rock drainage and ambient river water. *Geochim. Cosmochim. Acta* **2008**, 72 (2),  
581 311–328 DOI: 10.1016/j.gca.2007.11.013.
- 582 (37) Nelson, J.; Wasylenki, L.; Bargar, J. R.; Brown, G. E.; Maher, K. Effects of surface  
583 structural disorder and surface coverage on isotopic fractionation during Zn(II)  
584 adsorption onto quartz and amorphous silica surfaces. *Geochim. Cosmochim. Acta*  
585 **2017**, 215, 354–376 DOI: 10.1016/j.gca.2017.08.003.

- 586 (38) Dong, S.; Wasylenki, L. E. Zinc isotope fractionation during adsorption to calcite at high  
587 and low ionic strength. *Chem. Geol.* **2016**, *447*, 70–78 DOI:  
588 10.1016/j.chemgeo.2016.10.031.
- 589 (39) Guinoiseau, D.; Gélabert, A.; Moureau, J.; Louvat, P.; Benedetti, M. F. Zn Isotope  
590 Fractionation during Sorption onto Kaolinite. *Environ. Sci. Technol.* **2016**, *50* (4), 1844–  
591 1852 DOI: 10.1021/acs.est.5b05347.
- 592 (40) Jouvin, D.; Louvat, P.; Juillot, F.; Maréchal, C. N.; Benedetti, M. F. Zinc isotopic  
593 fractionation: Why organic matters. *Environ. Sci. Technol.* **2009**, *43* (15), 5747–5754  
594 DOI: 10.1021/es803012e.
- 595 (41) Houben, D.; Sonnet, P.; Tricot, G.; Mattielli, N.; Couder, E.; Opfergelt, S. Impact of root-  
596 induced mobilization of zinc on stable Zn isotope variation in the soil-plant system.  
597 *Environ. Sci. Technol.* **2014**, *48* (14), 7866–7873 DOI: 10.1021/es5002874.
- 598 (42) Couder, E.; Mattielli, N.; Drouet, T.; Smolders, E.; Delvaux, B.; Iserentant, A.; Meeus, C.;  
599 Maerschalk, C.; Opfergelt, S.; Houben, D. Transpiration flow controls Zn transport in  
600 Brassica napus and Lolium multiflorum under toxic levels as evidenced from isotopic  
601 fractionation. *Comptes Rendus - Geosci.* **2015**, *347* (7–8), 386–396 DOI:  
602 10.1016/j.crte.2015.05.004.
- 603 (43) Kirk, G. J. D.; Bajita, J. B. Root-induced iron oxidation, pH changes and zinc solubilization  
604 in the rhizosphere of lowland rice. *New Phytol.* **1995**, *131* (1), 129–137 DOI:  
605 10.1111/j.1469-8137.1995.tb03062.x.
- 606 (44) Aucour, A. M.; Bedell, J. P.; Queyron, M.; Magnin, V.; Testemale, D.; Sarret, G.  
607 Dynamics of Zn in an urban wetland soil-plant system: Coupling isotopic and EXAFS  
608 approaches. *Geochim. Cosmochim. Acta* **2015**, *160*, 55–69 DOI:  
609 10.1016/j.gca.2015.03.040.
- 610 (45) Tang, Y. T.; Cloquet, C.; Deng, T. H. B.; Sterckeman, T.; Echevarria, G.; Yang, W. J.;  
611 Morel, J. L.; Qiu, R. L. Zinc Isotope Fractionation in the Hyperaccumulator *Noccaea*  
612 *caerulescens* and the Nonaccumulating Plant *Thlaspi arvense* at Low and High Zn  
613 Supply. *Environ. Sci. Technol.* **2016**, *50* (15), 8020–8027 DOI: 10.1021/acs.est.6b00167.

- 614 (46) Arnold, T.; Kirk, G. J. D.; Wissuwa, M.; Frei, M.; Zhao, F.-J.; Mason, T. F. D.; Weiss, D. J.  
615 Evidence for the mechanisms of zinc uptake by rice using isotope fractionation. *Plant.*  
616 *Cell Environ.* **2010**, *33* (3), 370–381 DOI: 10.1111/j.1365-3040.2009.02085.x.
- 617 (47) Arnold, T.; Markovic, T.; Kirk, G. J. D.; Schönbacher, M.; Rehkämper, M.; Zhao, F. J.;  
618 Weiss, D. J. Iron and zinc isotope fractionation during uptake and translocation in rice  
619 (*Oryza sativa*) grown in oxic and anoxic soils. *Comptes Rendus - Geosci.* **2015**, *347* (7–8),  
620 397–404 DOI: 10.1016/j.crte.2015.05.005.
- 621 (48) Houben, D.; Sonnet, P. Zinc mineral weathering as affected by plant roots. *Appl.*  
622 *Geochemistry* **2012**, *27* (8), 1587–1592 DOI: 10.1016/j.apgeochem.2012.05.004.
- 623 (49) Belon, E.; Boisson, M.; Deportes, I. Z.; Eglin, T. K.; Feix, I.; Bispo, A. O.; Galsomies, L.;  
624 Leblond, S.; Guellier, C. R. An inventory of trace elements inputs to French agricultural  
625 soils. *Sci. Total Environ.* **2012**, *439*, 87–95 DOI: 10.1016/j.scitotenv.2012.09.011.
- 626 (50) Schultheiß, U.; Döhler, H.; Roth, U.; Eckel, H.; Kühnen, V.; Goldbach, H.; Wilcke, W.;  
627 Uihlein, A.; Früchtenicht, K.; Steffens, G. Schwermetallbilanzen in  
628 Tierproduktionsbetrieben. In *VDLUFA-Schriftenreihe 59*; VDLUFA-Verlag, Bonn:  
629 Saarbrücken, 2003; pp 232–243.
- 630 (51) Keller, A.; Schulin, R. Modelling heavy metal and phosphorus balances for farming  
631 systems. *Nutr. Cycl. Agroecosystems* **2003**, *66* (3), 271–284 DOI:  
632 10.1023/A:1024410126924.
- 633 (52) Lobe, I.; Wilcke, W.; Kobža, J.; Zech, W. Heavy metal contamination of soils in Northern  
634 Slovakia. *Zeitschrift Fur Pflanzenernahrung Und Bodenkd.* **1998**, *161* (5), 541–546 DOI:  
635 10.1002/jpln.1998.3581610507.
- 636 (53) Wilcke, W.; Kretschmar, S.; Bundt, M.; Saborío, G.; Zech, W. Depth distribution of  
637 aluminum and heavy metals in soils of Costa Rican coffee cultivation areas. *J. Plant*  
638 *Nutr. Soil Sci.* **2000**, *163* (5), 499–502 DOI: 10.1002/1522-  
639 2624(200010)163:5<499::AID-JPLN499>3.0.CO;2-8.
- 640 (54) Imseng, M.; Wiggerhauser, M.; Keller, A.; Müller, M.; Rehkämper, M.; Murphy, K.;  
641 Kreissig, K.; Frossard, E.; Wilcke, W.; Bigalke, M. Fate of Cd in agricultural soils: A stable

- 642 isotope approach to anthropogenic impact, soil formation and soil-plant cycling.  
643 *Environ. Sci. Technol.* **2018**, *52* (4), acs.est.7b05439 DOI: 10.1021/acs.est.7b05439.
- 644 (55) St. Arnaud, R. J.; Stewart, J. W. B.; Frossard, E. Application of the “Pedogenic Index” to  
645 soil fertility studies, Saskatchewan. *Geoderma* **1988**, *43* (1), 21–32 DOI: 10.1016/0016-  
646 7061(88)90052-3.
- 647 (56) Jobbagy, E. G.; Jackson, R. B. The distribution of soil nutrients with depth : Global  
648 patterns of the imprint of plants. *Biogeochemistry* **2001**, *53*, 51–77.
- 649 (57) *World reference base for soil resources 2014: International soil classification system for*  
650 *naming soils and creating legends for soil maps*; World soil resources reports; FAO:  
651 Rome, 2014.
- 652 (58) Caldelas, C.; Dong, S.; Araus, J. L.; Jakob Weiss, D. Zinc isotopic fractionation in  
653 *Phragmites australis* in response to toxic levels of zinc. *J. Exp. Bot.* **2011**, *62* (6), 2169–  
654 2178 DOI: 10.1093/jxb/erq414.
- 655 (59) Wiggerhauser, M.; Bigalke, M.; Imseng, M.; Keller, A.; Archer, C.; Wilcke, W.; Frossard,  
656 E. Zinc isotope fractionation during grain filling of wheat and a comparison of Zn and  
657 Cd isotope ratios in identical soil-plant systems. *New Phytol.* **2018**.
- 658 (60) Jochum, K. P.; Nohl, U.; Herwig, K.; Lammel, E.; Stoll, B.; Hofmann, A. W. GeoReM: A  
659 new geochemical database for reference materials and isotopic standards. *Geostand.*  
660 *Geoanalytical Res.* **2005**, *29* (3), 333–338 DOI: 10.1111/j.1751-908X.2005.tb00904.x.
- 661 (61) Pribyl, D. W. A critical review of the conventional SOC to SOM conversion factor.  
662 *Geoderma* **2010**, *156* (3–4), 75–83 DOI: 10.1016/j.geoderma.2010.02.003.
- 663 (62) Groenenberg, J. E.; Koopmans, G. F.; Comans, R. N. J. Uncertainty analysis of the  
664 nonideal competitive adsorption - Donnan model: Effects of dissolved organic matter  
665 variability on predicted metal speciation in soil solution. *Environ. Sci. Technol.* **2010**, *44*  
666 (4), 1340–1346 DOI: 10.1021/es902615w.
- 667 (63) Ren, Z.-L.; Tella, M.; Bravin, M. N.; Comans, R. N. J.; Dai, J.; Garnier, J.-M.; Sivry, Y.;  
668 Doelsch, E.; Straathof, A.; Benedetti, M. F. Effect of dissolved organic matter  
669 composition on metal speciation in soil solutions. *Chem. Geol.* **2015**, *398*, 61–69 DOI:

- 670 10.1016/j.chemgeo.2015.01.020.
- 671 (64) Brimhall, G. H.; Chadwick, O. A.; Lewis, C. J.; Compston, W.; Williams, I. S.; Danti, K. J.;  
672 Dietrich, W. E.; Power, M. E.; Hendricks, D.; Bratt, J. Deformational mass transport and  
673 invasive processes in soil evolution. *Science* **1992**, *255* (5045), 695–702 DOI:  
674 10.1126/science.255.5045.695.
- 675 (65) Kösel, M. Der Einfluss von Relief und periglazialen Deckschichten auf die Bodenbildung  
676 im mittleren Rheingletschergebiet von Oberschwaben, 1996.
- 677 (66) Völkel, J.; Mahr, A. Neue Befunde zum Alter der periglazialen Deckschichten im  
678 Vorderen Bayerischen Wald. *Zeitschrift für Geomorphol.* **1997**, *41* (1), 131–137.
- 679 (67) Mailänder, R.; Veit, H. Periglacial cover-beds on the Swiss Plateau: Indicators of soil,  
680 climate and landscape evolution during the Late Quaternary. *Catena* **2001**, *45* (4), 251–  
681 272 DOI: 10.1016/S0341-8162(01)00151-5.
- 682 (68) Rauch, J. N.; Pacyna, J. M. Earth's global Ag, Al, Cr, Cu, Fe, Ni, Pb, and Zn cycles. *Global*  
683 *Biogeochem. Cycles* **2009**, *23* (2), n/a-n/a DOI: 10.1029/2008GB003376.
- 684 (69) Emmanuel, S.; Levenson, Y. Limestone weathering rates accelerated by micron-scale  
685 grain detachment. *Geology* **2014**, *42* (9), 751–754 DOI: 10.1130/G35815.1.
- 686 (70) Buss, H. L.; Sak, P. B.; Webb, S. M.; Brantley, S. L. Weathering of the Rio Blanco quartz  
687 diorite, Luquillo Mountains, Puerto Rico: Coupling oxidation, dissolution, and  
688 fracturing. *Geochim. Cosmochim. Acta* **2008**, *72* (18), 4488–4507 DOI:  
689 10.1016/j.gca.2008.06.020.
- 690 (71) White, A. F.; Buss, H. L. Natural weathering rates of silicate minerals. In *Treatise on*  
691 *Geochemistry*; Elsevier, 2014; pp 115–155.
- 692 (72) EFSA. *Scientific Opinion on the potential reduction of the currently authorised maximum*  
693 *zinc content in complete feed*; 2014; Vol. 12.
- 694 (73) von Steiger, B.; Baccini, P. *Regionale Stoffbilanzierung von landwirtschaftlichen Böden*  
695 *mit messbarem Ein- und Austrag. Bericht des Nationalen Forschungsprogramms*  
696 *“Boden” 38*; Liebefele-Bern, 1990.

- 697 (74) Wilkinson, J. J.; Weiss, D. J.; Mason, T. F. D.; Coles, B. J. Zinc isotope variation in  
698 hydrothermal systems: Preliminary evidence from the Irish midlands ore field. *Econ.*  
699 *Geol.* **2005**, *100* (3), 583–590 DOI: 10.2113/gsecongeo.100.3.583.
- 700 (75) Cloquet, C.; Carignan, J.; Lehmann, M. F.; Vanhaecke, F. Variation in the isotopic  
701 composition of zinc in the natural environment and the use of zinc isotopes in  
702 biogeosciences: A review. *Anal. Bioanal. Chem.* **2008**, *390* (2), 451–463 DOI:  
703 10.1007/s00216-007-1635-y.
- 704 (76) Luck JM; Othman DB; Albarède F; Telouk P. Pb, Zn and Cu isotopic variations and trace  
705 elements in rain. In *GEOCHEMISTRY OF THE EARTH'S SURFACE*; A.A. Balkema, 1999; pp  
706 199–202.
- 707 (77) Dong, S.; Weiss, D. J.; Strekopytov, S.; Kreissig, K.; Sun, Y.; Baker, A. R.; Formenti, P.  
708 Stable isotope ratio measurements of Cu and Zn in mineral dust (bulk and size  
709 fractions) from the Taklimakan Desert and the Sahel and in aerosols from the eastern  
710 tropical North Atlantic Ocean. *Talanta* **2013**, *114*, 103–109 DOI:  
711 10.1016/j.talanta.2013.03.062.
- 712 (78) Cloquet, C.; Carignan, J.; Libourel, G. Isotopic composition of Zn and Pb atmospheric  
713 depositions in an urban/periurban area of northeastern France. *Environ. Sci. Technol.*  
714 **2006**, *40* (21), 6594–6600 DOI: 10.1021/es0609654.
- 715 (79) Gioia, S.; Weiss, D.; Coles, B.; Arnold, T.; Babinski, M. Accurate and Precise Zinc Isotope  
716 Ratio Measurements in Urban Aerosols. *Anal. Chem.* **2008**, *80* (24), 9776–9780.
- 717 (80) Bryan, A. L.; Dong, S.; Wilkes, E. B.; Wasylenki, L. E. Zinc isotope fractionation during  
718 adsorption onto Mn oxyhydroxide at low and high ionic strength. *Geochim.*  
719 *Cosmochim. Acta* **2015**, *157*, 182–197 DOI: 10.1016/j.gca.2015.01.026.
- 720 (81) Hacisalihoglu, G.; Hart, J. J.; Kochian, L. V. High- and low-affinity zinc transport systems  
721 and their possible role in zinc efficiency in bread wheat. *Plant Physiol.* **2001**, *125* (1),  
722 456–463 DOI: 10.1104/pp.125.1.456.
- 723 (82) Jouvin, D.; Weiss, D. J.; Mason, T. F. M.; Bravin, M. N.; Louvat, P.; Zhao, F.; Ferec, F.;  
724 Hinsinger, P.; Benedetti, M. F. Stable isotopes of Cu and Zn in higher plants: Evidence

- 725 for Cu reduction at the root surface and two conceptual models for isotopic  
726 fractionation processes. *Environ. Sci. Technol.* **2012**, *46* (5), 2652–2660 DOI:  
727 10.1021/es202587m.
- 728 (83) Aucour, A. M.; Pichat, S.; MacNair, M. R.; Oger, P. Fractionation of stable zinc isotopes  
729 in the zinc hyperaccumulator *Arabidopsis halleri* and nonaccumulator *Arabidopsis*  
730 *petraea*. *Environ. Sci. Technol.* **2011**, *45* (21), 9212–9217 DOI: 10.1021/es200874x.
- 731 (84) Weiss, D. J.; Mason, T. F. D.; Zhao, F. J.; Kirk, G. J. D.; Coles, B. J.; Horstwood, M. S. A.  
732 Isotopic discrimination of zinc in higher plants. *New Phytol.* **2005**, *165* (3), 703–710  
733 DOI: 10.1111/j.1469-8137.2004.01307.x.
- 734 (85) Goldschmidt, V. M. The principles of distribution of chemical elements in minerals and  
735 rocks. The seventh Hugo Müller Lecture, delivered before the Chemical Society on  
736 March 17th, 1937. *J. Chem. Soc.* **1937**, *0* (0), 655–673 DOI: 10.1039/JR9370000655.
- 737 (86) Reimann, C.; Englmaier, P.; Flem, B.; Gough, L.; Lamothe, P.; Nordgulen, Ø.; Smith, D.  
738 Geochemical gradients in soil O-horizon samples from southern Norway: Natural or  
739 anthropogenic? *Appl. Geochemistry* **2009**, *24* (1), 62–76 DOI:  
740 10.1016/j.apgeochem.2008.11.021.
- 741 (87) Reimann, C.; Arnoldussen, A.; Englmaier, P.; Filzmoser, P.; Finne, T. E.; Garrett, R. G.;  
742 Koller, F.; Nordgulen, Ø. Element concentrations and variations along a 120-km  
743 transect in southern Norway – Anthropogenic vs. geogenic vs. biogenic element  
744 sources and cycles. *Appl. Geochemistry* **2007**, *22* (4), 851–871 DOI:  
745 10.1016/j.apgeochem.2006.12.019.
- 746 (88) Imseng, M.; Wiggnerhauser, M.; Keller, A.; Müller, M.; Rehkämper, M.; Murphy, K.;  
747 Kreissig, K.; Frossard, E.; Wilcke, W.; Bigalke, M. Towards an understanding of the Cd  
748 isotope fractionation during transfer from the soil to the cereal grain. *Environ. Pollut.*  
749 **2019**, *244*, 834–844 DOI: 10.1016/J.ENVPOL.2018.09.149.
- 750 (89) Pahlsson, A.-M. B. Toxicity of heavy metals (Zn, Cu, Cd, Pb) to vascular plants. *Water.*  
751 *Air. Soil Pollut.* **1989**, *47* (3–4), 287–319 DOI: 10.1007/BF00279329.
- 752 (90) Santorufo, L.; Van Gestel, C. A. M.; Rocco, A.; Maisto, G. Soil invertebrates as

753 bioindicators of urban soil quality. *Environ. Pollut.* **2012**, *161*, 57–63 DOI:  
754 10.1016/j.envpol.2011.09.042.

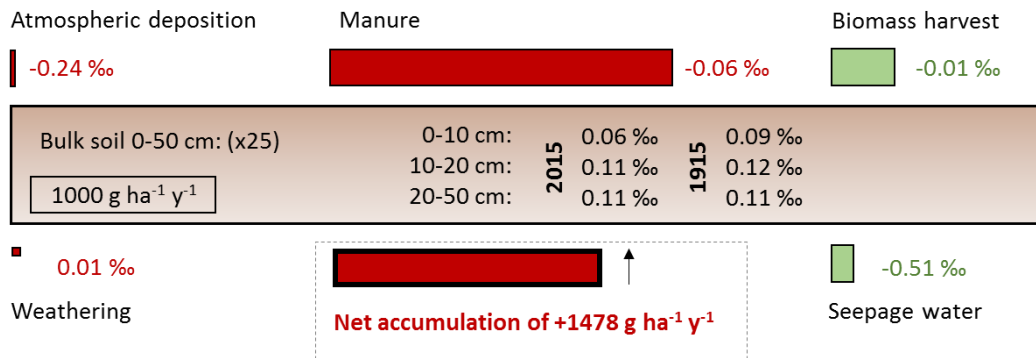
755 (91) Yuan-peng, W.; Ji-yan, S. H. I.; Qi, L. I. N.; Xin-cai, C.; Ying-xu, C. Heavy metal availability  
756 and impact on activity of soil microorganisms along a Cu / Zn contamination gradient. *J.*  
757 *Environ. Sci.* **2007**, *19*, 848–853.

758

759

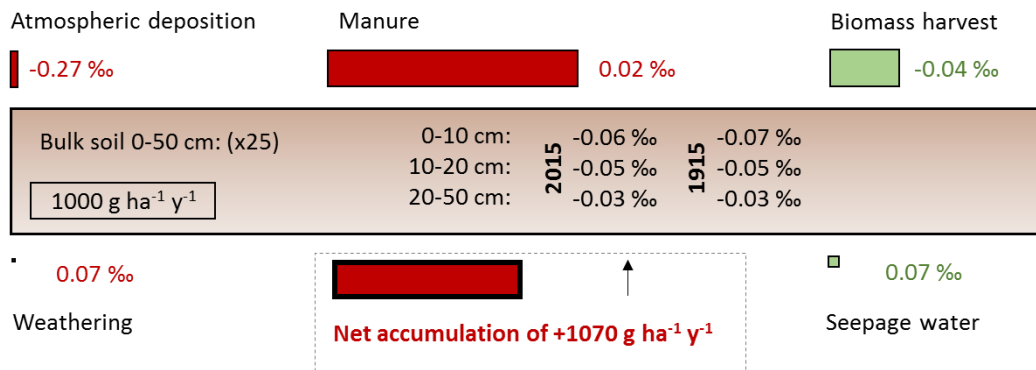
760

### Tänikon (a)



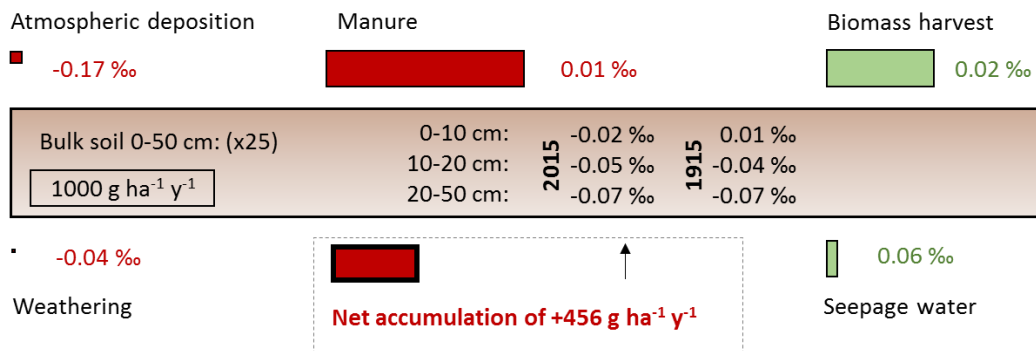
761

### Ebikon (b)



762

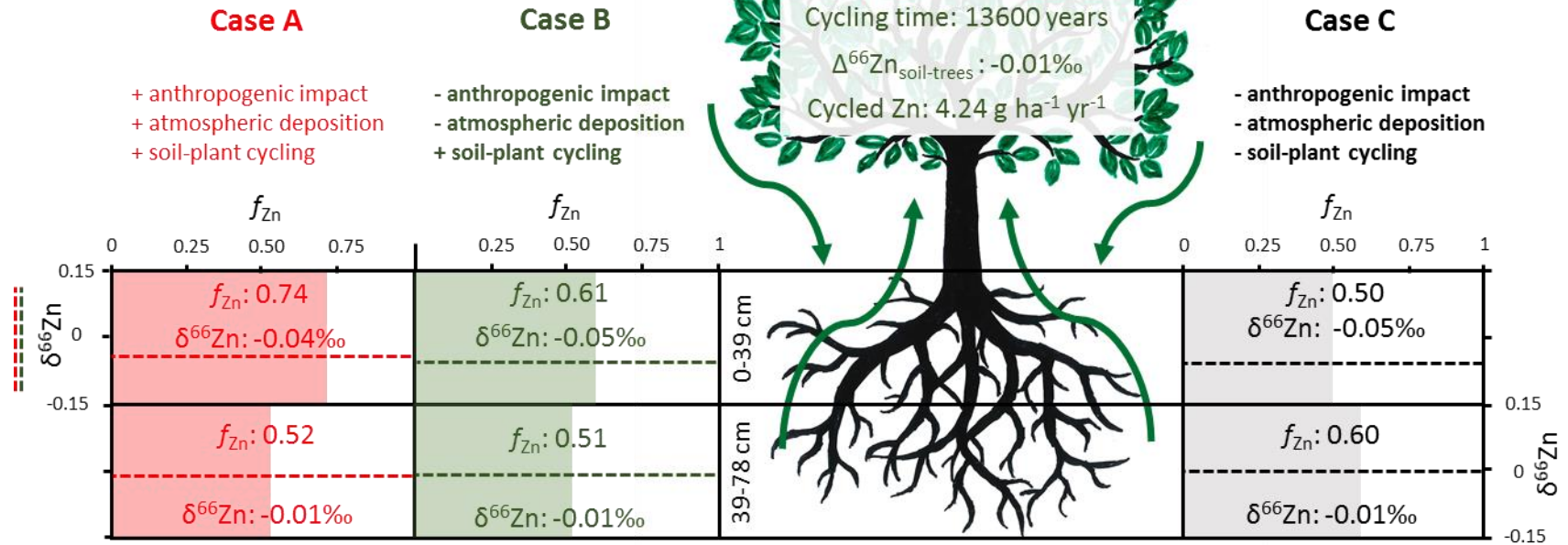
### Ependes (c)



763

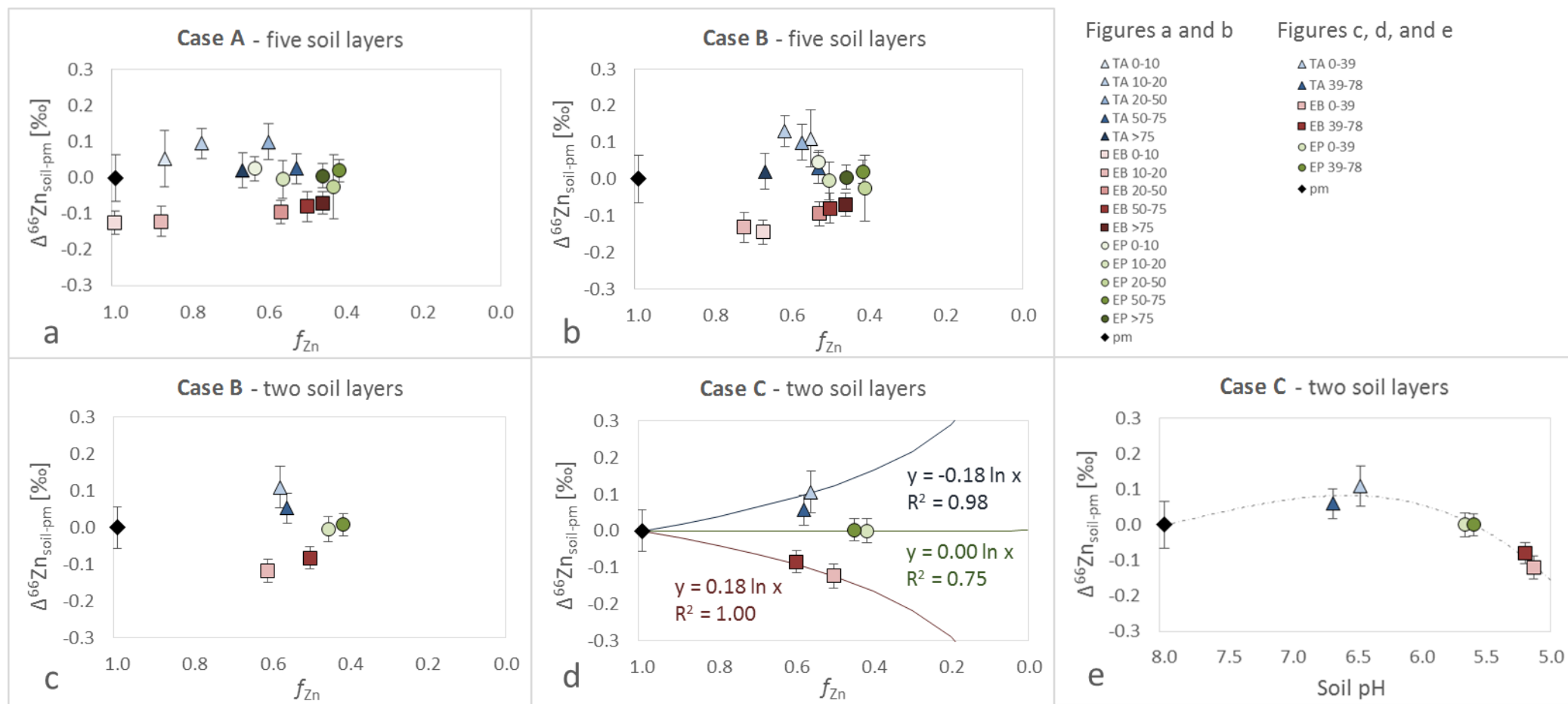
764 Figure 1. Zinc mass balance of the three grassland sites Tänikon (a), Ebikon (b), and Ependes (c) in  
 765 Switzerland for one hydrological year (May 2014 – May 2015). System inputs are shown in red;  
 766 system losses are shown in green. Sizes of the boxes are proportional to the size of Zn fluxes  
 767 (compared to the reference box of 1000 g Zn ha<sup>-1</sup> yr<sup>-1</sup>). Sizes of the bulk soil boxes had to be reduced  
 768 and would be 25x bigger to proportionally represent real Zn stocks of the soils. Net accumulations  
 769 represent the mass balance values after one hydrological year. The  $\delta^{66}\text{Zn}$  values of inputs and  
 770 outputs are given next to the boxes. The  $\delta^{66}\text{Zn}$  values of the three soil layers are given in the soil  
 771 boxes; 2015 values were measured, 1915 values were calculated with the “anthropogenic impact  
 772 model”.

# Ebikon



773

774 Figure 2. Results of the *anthropogenic and atmospheric impact* and the *soil-plant cycling model* at Ebikon. **Case A** in red gives the remaining Zn fractions ( $f_{\text{Zn}} =$   
 775  $\tau_{\text{Zn}} + 1$ ) and the isotope compositions ( $\delta^{66}\text{Zn}_{\text{soil}}$ ) of the two soil-layers (0–39 and 39–78 cm) in the year 2015 and includes the anthropogenic impact, former  
 776 atmospheric deposition, and soil-plant cycling. **Case B** in green gives the  $f_{\text{Zn}}$  and  $\delta^{66}\text{Zn}_{\text{soil}}$  values after application of the *anthropogenic and atmospheric impact*,  
 777 and *soil-plant cycling model* in the year 1915, without anthropogenic impact, without former atmospheric deposition but with soil-plant cycling. **Case C** in black  
 778 gives  $f_{\text{Zn}}$  and  $\delta^{66}\text{Zn}_{\text{soil}}$  values after application of the *anthropogenic and atmospheric impact* and the *soil-plant cycling model* in the year 1915, without  
 779 anthropogenic impact, without former atmospheric deposition and without soil-plant cycling.  $f_{\text{Zn}}$  values are illustrated with red, green and grey shading,  
 780 respectively, and the  $\delta^{66}\text{Zn}_{\text{soil}}$  values are indicated with dotted horizontal lines.



781

782 Figure 3. Relationship of the apparent isotope fractionation between soils and parent materials ( $\Delta^{66}\text{Zn}_{\text{soil-pm}}$ ) with (a-d) the remaining Zn fraction in soils ( $f_{\text{Zn}} = \tau_{\text{Zn}}$   
 783 values + 1) as well as (e) the soil pH, for Tännikon ( $\blacktriangle$ ), Ebikon ( $\blacksquare$ ) and Ependes ( $\bullet$ ). (a) **Case A**: current values in the year 2015 with anthropogenic impact, with  
 784 former atmospheric deposition, and with soil-plant cycling. (b & c) **Case B**: values in the year 1915 without anthropogenic impact and former atmospheric  
 785 inputs but with soil-plant cycling. (d and e) **Case C**: values in the year 1915 without anthropogenic impact and former atmospheric inputs and without soil-plant  
 786 cycling. Rayleigh fractionation factors for soil formation in (d) were -0.18, -0.18, and 0.00 at Tännikon, Ebikon, and Ependes, respectively. Soil pH values in (e)  
 787 were measured by the NABO in 1985<sup>9</sup> and the dotted line is for illustration purpose only and does not represent a model.